PHYSICAL REVIEW E **69**, 011502 (2004)

Density and temperature effects on the orientational and dielectric properties of supercritical water

E. Guàrdia*
Departament de Física i Enginyeria Nuclear, Universitat Politècnica de Catalunya, B4-205 Campus Nord,
08034 Barcelona, Catalonia, Spain

J. Martí †
Departament de Física i Enginyeria Nuclear, Universitat Politècnica de Catalunya. B5-206 Campus Nord,
08034 Barcelona, Catalonia, Spain

(Received 25 April 2003; published 27 January 2004)

The influence of temperature and density changes on the reorientational motions and dielectric properties of supercritical water is investigated by molecular dynamics simulations. A rigid simple point charged potential has been used to model water-water interactions. This model has revealed to be very satisfactory to reproduce thermodynamic, diffusive, and static dielectric properties of supercritical water. Reorientation times of water molecules have been computed along specific molecular directions and compared with available experimental data. The imaginary part of the frequency dependent dielectric constant, spectral densities of states, and residence times of water molecules in their first hydration shells are also evaluated.

DOI: 10.1103/PhysRevE.69.011502 PACS number(s): 61.25.Em, 31.15.Qg

I. INTRODUCTION

The study of the behavior of fluids beyond the critical point has revealed to be of increasing interest in the last decades [1]. Supercritical fluids are able to dissolve nonvolatile solids as many liquids do [2], and also to help the production of new materials at mild and moderated thermodynamic conditions. Supercritical water (SCW) has been a subject of study during past several decades, from the experimental [3–10], theoretical [11], and computational [12–21] points of view. The properties of liquid water are very different from those of most liquids [22], mainly due to the existence of the hydrogen bond (HB) network. Such tetrahedral network is partially broken in supercritical states [19] and consequently the macroscopic properties of SCW are radically different from those of the liquid state. For instance, oil does not mix with liquid water but mixes with SCW. In ambient conditions ions dissolve well in water but they are unable to dissolve in SCW. In addition, SCW shows a compressibility larger than dilute gases which produces transport properties in between of those of liquids and gases. The combination of all these unique properties makes SCW as a good medium for reaction and separation processes in general, and especially for the oxidation of organic wastes.

The aim of this work is the study of orientational and dielectric properties of SCW in terms of temperature and density variations. In a previous work a detailed density dependence analysis was performed [23]. The computed density behavior of reorientational and Debye dielectric characteristic times are in overall agreement with NMR [10] and microwave data [24]. However discrepancies between experimental and computer simulation results [23] arise when the low-density range of the dielectric relaxation time is considered. Similar discrepancies were also observed by other authors [25–27]. Here we are interested in the temperature dependence of orientational and spectroscopic properties for a wide range of densities. We will explain the technical details of our simulations in Sec. II and check the validity of the potential model employed in Sec. III. The main results concerning orientational properties, dielectric and spectroscopic properties and residence times of water molecules are reported in Secs. IV–VI. We conclude in Sec. VII.

II. COMPUTATIONAL METHODS

A series of molecular dynamics (MD) simulations along isotherms of $T=650$, 720, and 870 K, and densities between $\rho=0.7$ and 0.01 $\mathrm{g\,cm^{-3}}$ have been performed. The extended simple point charge (SPC/E) water model has been assumed in all simulations [28]. In this rigid model, the molecular dipole moment of water is $\mu=2.35$ D and the critical point of the model [29] is $T_c=640$ K, $\rho_c=0.29\ \mathrm{g\,cm^{-3}}$, $P_c=160$ bars. This is very close to the experimental critical point of water, i.e., $T_c=647.13$ K, $\rho_c=0.322\ \mathrm{g\,cm^{-3}}$, $P_c=220.55$ bars. Such a model reproduces very accurately many structural and dynamic properties of liquid water [30,31].

Our simulated systems were composed of 256 water molecules placed in a cubic box, with appropriate box lengths for each density. Periodic boundary conditions along the three spatial directions have been taken. Short ranged forces were truncated at half the box length, whereas the Ewald summation rule with conducting boundary conditions was applied to account for Coulomb interactions. A Berendsen thermostat [32] was coupled to each system to control temperatures. The time step was of 2 fs in all simulation runs, which consisted of initial equilibration periods of 50 ps, followed by simulation runs of 2.5 ns to collect statistically meaningful properties.

III. RELIABILITY OF THE MODEL

In computer simulations of SCW a central issue to consider is the election of a good potential model, able to fairly

---

*Electronic address: elvira.guardia@upc.es
†Electronic address: jordi.marti@upc.es

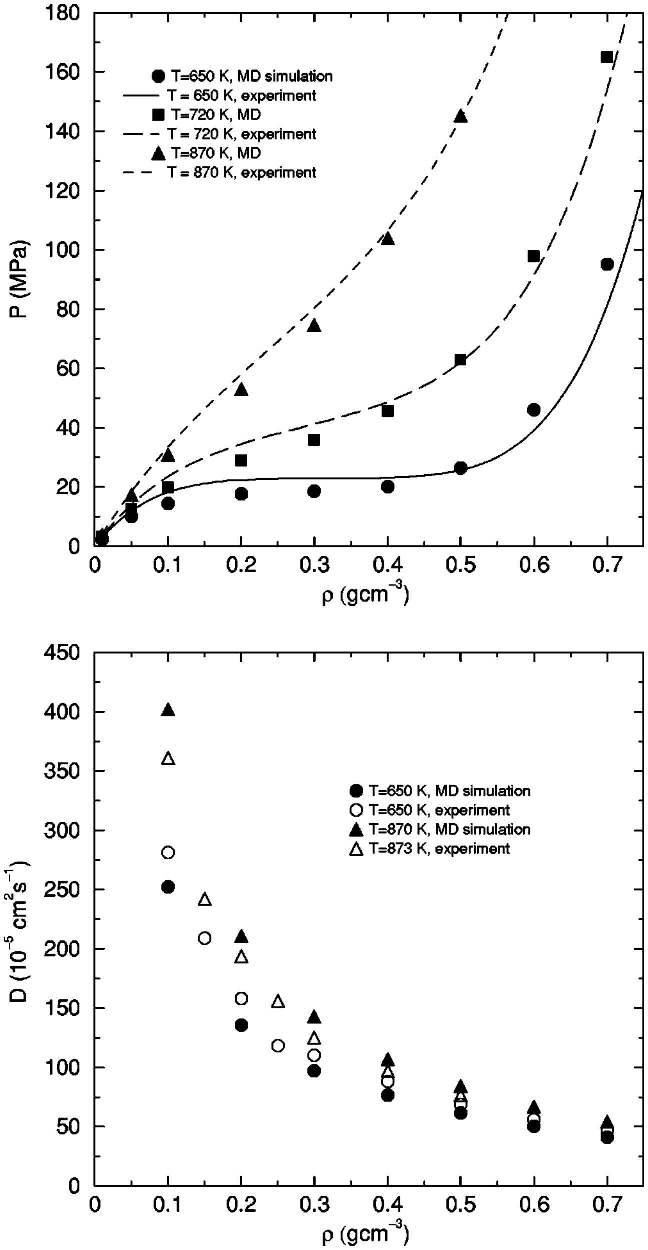

FIG. 1. Pressure and self-diffusion coefficients as a function of density at different temperatures. Experimental data are taken from Refs. [4] and [33].

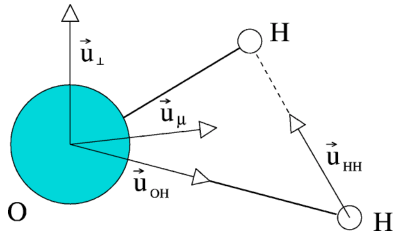

FIG. 2. Definition of unit vectors along relevant molecular directions.

reproduce experimental thermodynamic properties, structure and dynamics of the system. We have checked the reliability of the SPC/E model through the calculation of the pressure as a function of density at the three temperatures considered in this work, together with self-diffusion coefficients as a function of density at the two extremal temperatures (650 and 870 K). The results are shown in Fig. 1. We observe an overall good agreement between experimental data (from Ref. [33] for pressures and Ref. [4] for diffusion coefficients) and computer simulation results. Only some quantitative discrepancies can be seen concerning self-diffusion coefficients at densities below 0.3 $\mathrm{g\,cm^{-3}}$, where MD simulations clearly overemphasize diffusion coefficients at 650 K and, however, render values smaller than the experimental ones at 870 K. This effect is seen at all densities, but it is less important as density increases. We conclude that, despite some minor defects, the SPC/E model can reproduce reasonably well general trends of SCW such as pressure and diffusive behavior. In Sec. V we will include a comparison of experimental and MD static dielectric constants in terms of density and temperature dependence to further demonstrate the reliability of the model.

IV. REORIENTATIONAL MOTIONS

The study of reorientational motions has been performed by means of a series of time correlation functions $C_{l,\alpha}(t)$ defined as follows:

$$C_{l,\alpha}(t)\equiv\langle P_l(\vec{u}_\alpha(t)\cdot\vec{u}_\alpha(0))\rangle \quad (l=1,2), \tag{1}$$

where P_l is the lth Legendre polynomial and $\vec{u}_\alpha$ is a unit vector along a given molecular direction. We employed four unit vectors: $\vec{u}_\mu$ defined along the molecular dipole moment direction, $\vec{u}_{OH}$ and $\vec{u}_{HH}$ along the O-H and H-H directions and $\vec{u}_\perp\equiv\vec{u}_\mu\times\vec{u}_{HH}$. Latter is perpendicular to the instantaneous molecular plane (Fig. 2). $C_{l,\alpha}(t)$ indicate how a given molecular direction (that of the dipole moment, of the O-H and H-H directions or the instantaneous direction perpendicular to the molecular plane) changes its orientation in time. On the other hand, $C_{1,\mu}(t)$ is directly related with dielectric relaxation measurements [34], whereas $C_{2,HH}(t)$ and $C_{2,OH}(t)$ are related with ^{1}H-^{1}H and ^{17}O-^{1}H dipolar relaxation NMR experiments, respectively [35].

We show $C_{l,\mu}(t)(l=1,2)$ at three densities and three temperatures in Fig. 3. The density behavior at 650 K was previously studied [23]. Here we can observe that SCW mimics such behavior at higher temperatures. In all cases the initial fast decay of $C_{l,\mu}(t)$ shows a tendency to be even faster as density is lowered, approaching the gaslike behavior. The second remarkable effect observed is the gradual formation of a "backscatteringlike" minimum, more pronounced in the $C_{1,\mu}(t)$ case and deeper as temperature increases, again a signature of the gas phase characteristics. Such oscillation in $C_{1,\alpha}(t)$ is known as the free rotor frequency [36]. As a general fact, we observe that the influence of temperature is stronger at high densities. In Fig. 4 we show $C_{l,OH}(t)$. In this case, the main trends are the same observed for $C_{l,\mu}(t)$ although we can see the appearance of long time tails in $C_{1,OH}(t)$ associated with the lowest densities. $C_{l,HH}(t)$ are qualitatively equivalent to those of $C_{l,OH}(t)$ and they are not

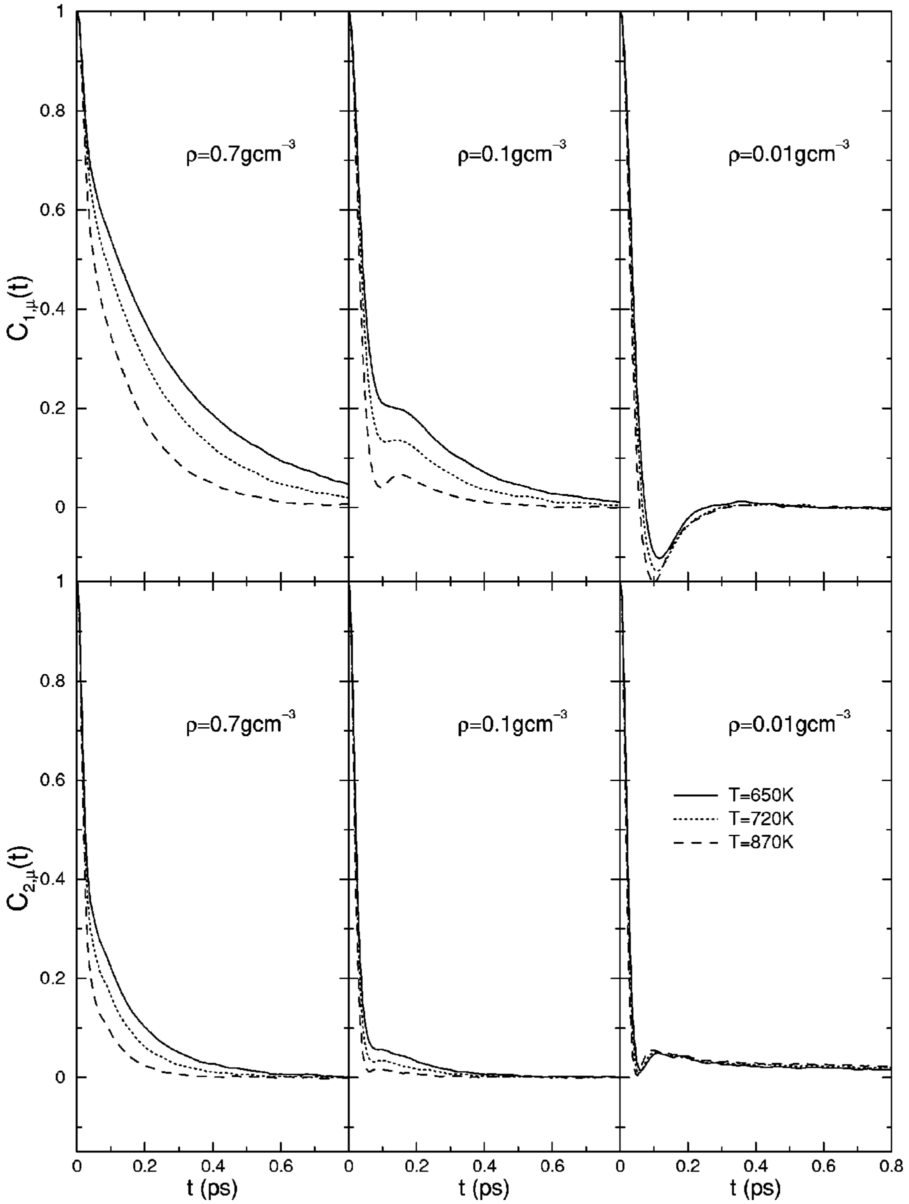

FIG. 3. Dipole moment correlation functions $C_{l,\alpha}(t)$ as a function of temperature at different densities.

reported. Finally, $C_{l,\perp}(t)$ (Fig. 5) reveals significative differences with the former at low densities: first, the backscatteringlike minimum is hardly seen, except for the lowest density and second the presence of long time tails at 0.01 $\mathrm{g\,cm^{-3}}$ is even clearer than in the $C_{1,OH}(t)$ case, suggesting the existence of low-frequency librational motions basically independent of temperature.

In order to shed some further light on the above results, it is convenient to calculate the time integrals of $C_{l,\mu}(t)(l=1,2)$, i.e., the so-called reorientational correlation times

$$\tau_{l,\alpha}=\int_0^\infty C_{l,\alpha}(t)dt \quad (l=1,2), \tag{2}$$

which basically indicate the mean time employed by a water molecule to rotate around a given molecular direction. In Fig. 6 we show $\tau_{l,\alpha}$ for all four molecular directions defined above. Two basic features can be distinguished: on the one hand, at intermediate and high densities, all four reorientational times behave in a similar fashion, rising for increasing densities. This happens at all three temperatures. Hence, we can see how the rotational motions are fastest at 870 K, i.e., times $\tau_{1,\alpha}$ and $\tau_{2,\alpha}$ are smaller than at 650 and 720 K. A way to explain this results is by means of the hydrogen bond populations at each state. It is known that large parts of the tetrahedral HB network existing in room temperature liquid water are broken in SCW [6]. This fact can be accounted through the calculation of HB percentages, which give about 1.6 bonds per water molecule at 673 K and 0.49 $\mathrm{g\,cm^{-3}}$ or 0.8 HB per water molecules at 773 K and 0.26 $\mathrm{g\,cm^{-3}}$, compared to 3.7 bonds for liquid water at ambient conditions [19]. Then, as temperature rises or density decreases, most of the HB disappear and, consequently, rotational motions of water molecules are likely to happen faster than in cool and/or dense systems. On the other hand, in the regime of low densities, both times are markedly higher than in the middle- and high-density regimes. Nevertheless, $\tau_{1,\mu}$ does not follow such tendency at low densities and instead de-

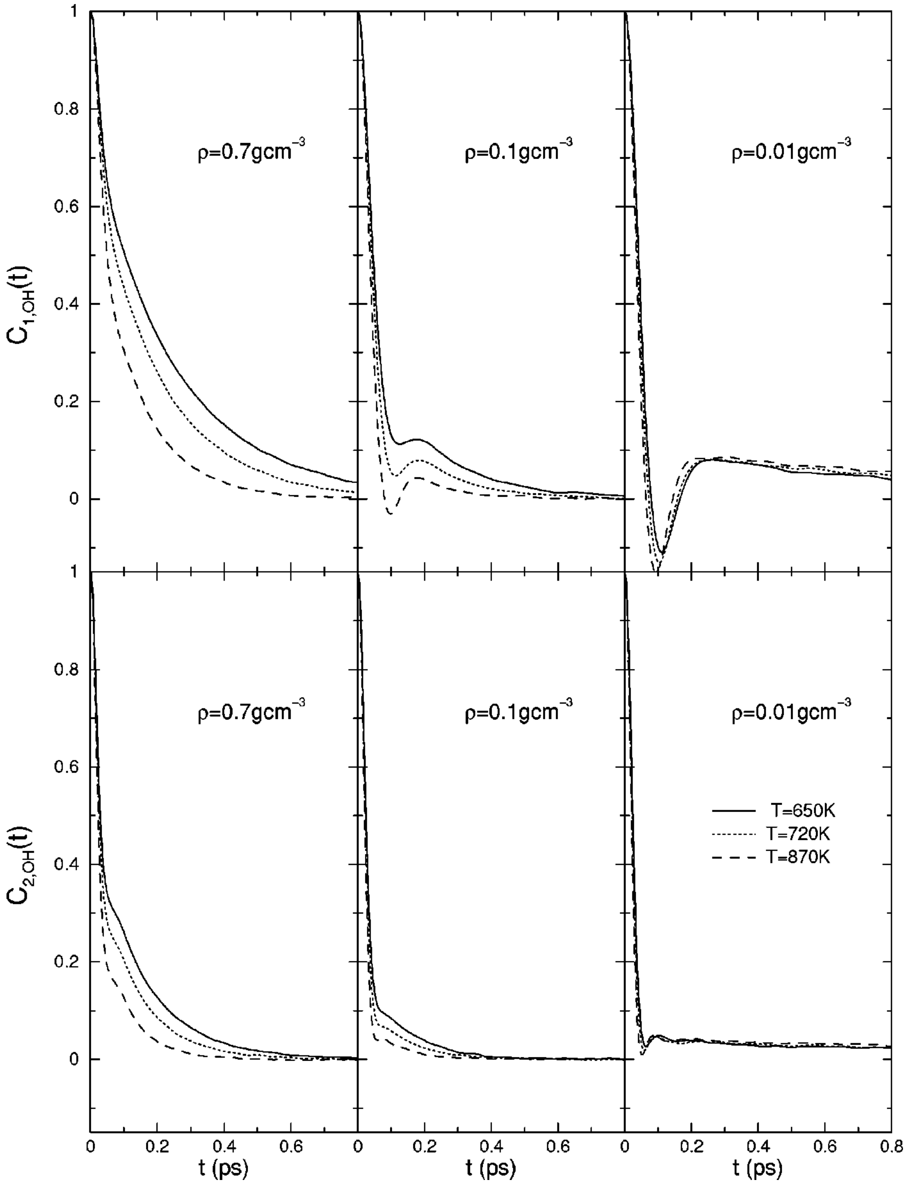

FIG. 4. Same as Fig. 3 for the $\vec{u}_{OH}$ direction.

creases to zero, giving an indication of the considerable strength of dipole-dipole interactions, even at low densities.

In particular, we find that $\tau_{1,\mu} > \tau_{1,OH} > \tau_{1,HH} > \tau_{1,\perp}$ for densities larger than 0.1 g cm^{-3} and $\tau_{1,\mu} < \tau_{1,OH} < \tau_{1,HH} < \tau_{1,\perp}$ below 0.1 g cm^{-3}. Such effect is seen at all temperatures. In the case of $\tau_{2,\alpha}$, we observe that the largest reorientational time corresponds to $\tau_{2,OH}$, followed by $\tau_{2,HH}$, $\tau_{2,\mu}$, and $\tau_{2,\perp}$. Furthermore, we observe that the computed time $\tau_{2,HH}$ reproduces qualitatively well the experimental NMR data reported by Matubayashi *et al.* [10] for heavy water. This reinforces the idea that the reorientational time measured in NMR experiments has to be attributed to the time calculated by means of the correlation function of the second Legendre polynomial. This fact has usually been employed in the interpretation of experiments together with the assumption of the isotropy of O-H and H-H water reorientations [35]. As it was pointed out before [23], this hypothesis fails in SCW at low densities. We clearly observe from Fig. 6 that O-H orientations are slower than H-H ones at all temperatures.

A significative difference between times $\tau_{1,\alpha}$ and $\tau_{2,\alpha}$ is their behavior at densities below 0.1 g cm^{-3}, while $\tau_{1,HH}$ differs of $\tau_{1,\perp}$ in about 20%, $\tau_{2,HH}$ and $\tau_{2,\perp}$ are roughly the same at all temperatures with a value very close to the experimental NMR data available (at 650 K). Then a nonisotropy of some selected molecular directions is again observed in the orientational order of SCW at low density. This fact should be attributed to the linearity of hydrogen-bonding in SCW at low densities [19], when the fluid suffers a gaslike behavior, also in its molecular rotational motions.

V. DIELECTRIC AND VIBRATIONAL SPECTRA

The static dielectric constant ε_0 of SCW has been computed at the three temperatures considered in this study as a function of density. For a system with long-range interactions treated by the Ewald method with conducting boundary conditions, ε_0 is given by [37]

$$\varepsilon_0 = \varepsilon_\infty + 3yG_k, \tag{3}$$

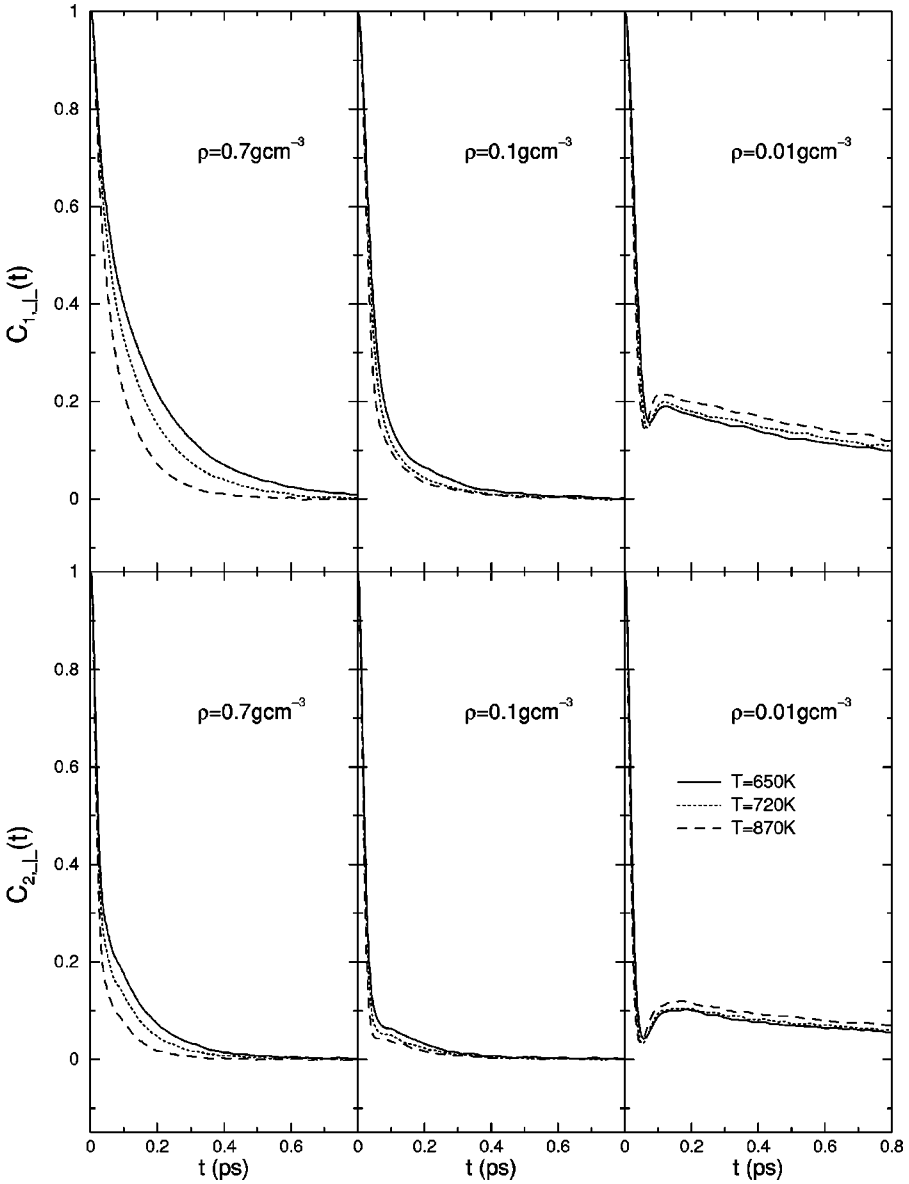

FIG. 5. Same as Fig. 3 for the $\vec{u}_\perp$ direction.

where ε_∞ is the dielectric constant at optical frequencies, $y=4\pi\rho\mu^2/9\ k_BT$ is the dimensionless dipolar strength, and G_k is the finite system Kirkwood g factor:

$$G_k=\frac{\langle M^2\rangle}{N\mu^2}, \tag{4}$$

which measures the equilibrium fluctuations of the total dipole moment of the sample $\vec{M}(t)=\Sigma_{i=1}^{N}\vec{\mu}_i(t)$. Because we are assuming rigid nonpolarizable molecules, in our case $\varepsilon_\infty=1$. The values of ε_0 found in this way are compared with experimental data in Fig. 7. A good overall agreement is found at all temperatures. As expected, ε_0 is lower for higher temperatures due to the reduction of the molecular ordering.

In order to have more detailed information of the dielectric properties of SCW, we have also computed the autocorrelation function for the total dipole moment of the system, defined as

$$\Phi(t)\equiv\frac{\langle\vec{M}(t)\cdot\vec{M}(0)\rangle}{\langle M^2(0)\rangle}, \tag{5}$$

which is the collective analogue of the single dipole moment autocorrelation function $C_{1,\mu}(t)$ [see Eq. (1)]. The comparison between $\Phi(t)$ and $C_{1,\mu}(t)$ is depicted in Fig. 8 for three selected densities (0.7, 0.1, and 0.01 g cm^{-3}) at 650, 720, and 870 K. This comparison gives an indication of the role played by cross correlations of dipole moments corresponding to distinct water molecules [34] as a function of temperature and density. As a general fact, we observe that the relaxation of $\Phi(t)$ is always slower than that of $C_{1,\mu}(t)$. In the regime of high density (0.7 g cm^{-3}), $\Phi(t)$ relaxes significantly slower than $C_{1,\mu}(t)$, as it corresponds to a condensed phase. In the range of intermediate density (0.1 g cm^{-3}), we still can observe how crossed correlations force $\Phi(t)$ to decay slower than $C_{1,\mu}(t)$. A hint of a relative minimum is already seen, especially at high temperatures. At low density

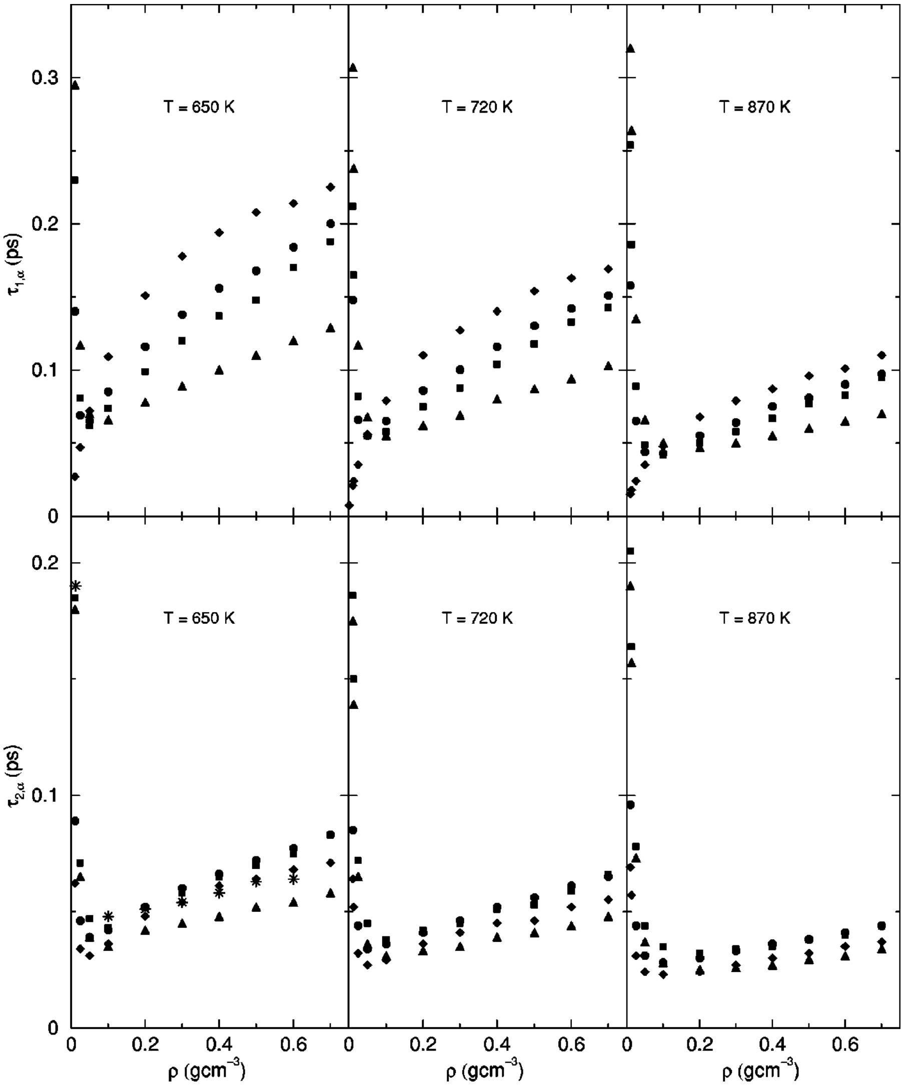

FIG. 6. Reorientational correlation times as a function of density at different temperatures. Diamonds—$\vec{u}_{\mu}$ direction, squares—$\vec{u}_{HH}$ direction, circles—$\vec{u}_{OH}$ direction, triangles—$\vec{u}_{\perp}$, stars—NMR data [10].

$(0.01\ \mathrm{g\,cm^{-3}})$, the relaxation rate of $\Phi(t)$ is very close to that of $C_{1,\mu}(t)$, i.e., both functions show the backscattering-like minimum already seen in Fig. 3.

Further insight on dielectric properties come from real and imaginary parts of the frequency-dependent dielectric constant, defined as

$$\varepsilon(\omega)=\varepsilon'(\omega)-i\varepsilon''(\omega). \tag{6}$$

If the Ewald summation technique is used to handle the long-range interactions, and conducting walls boundary conditions are assumed, the relation between $\varepsilon(\omega)$ and the total dipole moment correlation function is given by [39,40]

$$\varepsilon'(\omega)=\varepsilon_0-(\varepsilon_0-\varepsilon_\infty)\omega\int_0^\infty \Phi(t)\sin\omega t\,dt,$$

$$\varepsilon''(\omega)=(\varepsilon_0-\varepsilon_\infty)\omega\int_0^\infty \Phi(t)\cos\omega t\,dt. \tag{7}$$

Density and temperature influence on the imaginary part $\varepsilon''(\omega)$ are analyzed from Figs. 9 and 10. Concerning density dependence, we observe in Fig. 9 the existence of two broad bands centered at high (between 4900 and 5650 GHz) and low (between 550 and 950 GHz) frequencies. The low-frequency band appears basically at high densities and it is due to reorientational motions of the total dipole moment. As density is reduced such band shifts towards higher frequencies to virtually disappear in the very dilute system of $0.01\ \mathrm{g\,cm^{-3}}$. Instead, a high-frequency band associated with inertial rotations is observed in such low-density regime [23]. When temperature changes are considered (Fig. 10), the two main bands suffer spectral displacements in the following way. At the densities of 0.7 and $0.01\ \mathrm{g\,cm^{-3}}$, the dominant frequency band is shifted to higher values for increasing temperature, whereas the coexistence of the two frequency bands at $0.1\ \mathrm{g\,cm^{-3}}$ and 650 K progressively disappears as temperature increases and the free rotor band becomes dominant at 870 K.

After $\varepsilon(\omega)$ is known, the Debye relaxation time τ_D, which in the framework of the Debye theory of dielectric relaxation is defined as

$$\frac{\varepsilon(\omega)-\varepsilon_\infty}{\varepsilon_0-\varepsilon_\infty}=\frac{1}{1+i\omega\tau_D} \tag{8}$$

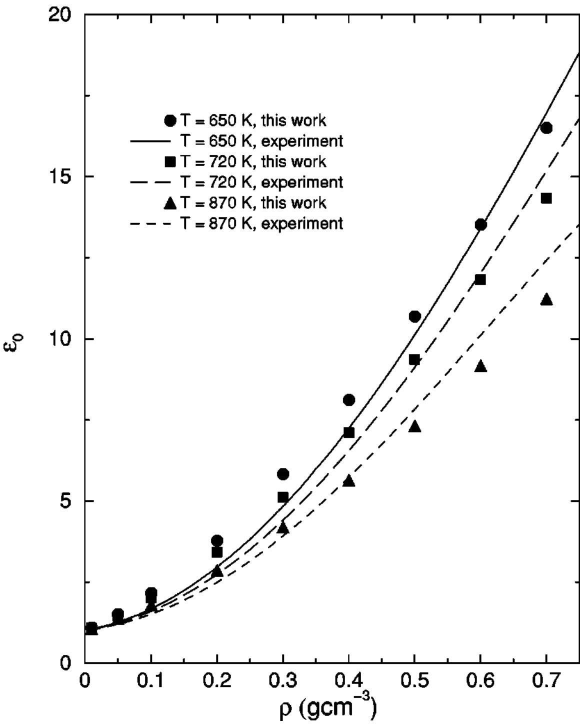

FIG. 7. Static dielectric constant as a function of density at different temperatures. Experimental data are obtained from Ref. [38].

can be obtained from the low-frequency behavior

$$\tau_D = \lim_{\omega\to 0} \frac{\varepsilon_0 - \varepsilon(\omega)}{i\omega[\varepsilon(\omega) - \varepsilon_\infty]}. \tag{9}$$

It can be shown that τ_D is the collective analog to $\tau_{1,\mu}$ [39,40]. As it can be seen from Fig. 11, the Debye relaxation times τ_D obtained from our MD simulations systematically decrease as density diminishes. The influence of ρ is significantly more important for τ_D than for the single dipole moment reorientational time $\tau_{1,\mu}$. On the other hand, the temperature increasing produces a reduction of both times τ_D and $\tau_{1,\mu}$, being especially relevant for τ_D. Further, the ratio $\tau_D/\tau_{1,\mu}$ which weighs the influence of the cross correlations on reorientations of the dipole moment is nearly constant and ~ 2 at densities larger than 0.2 $\mathrm{g\,cm^{-3}}$ and at all temperatures, approaching the unity for dilute low-density systems, as it happens for ideal gases.

A comparison of our findings with microwave experimental data [24] and other MD calculations [26] has been included in Fig. 11. We can observe that τ_D is reduced as density decreases for all MD simulations considered. On the contrary, experimental data indicate a clear increasing of τ_D at low densities. In the light of the present results, several conclusions can be obtained. First, there is an overall bad agreement between the microwave spectroscopy data of Okada *et al.* [24] and MD results, with some good accordance only for densities larger than 0.3 $\mathrm{g\,cm^{-3}}$. Second, such accordance is poorer as temperature increases. Third, several MD simulations using different types of potential models (see also Refs. [25–27]) produce results qualitatively similar for τ_D. Since computer simulations using different potential models basically agree, the explanation of the discrepancies at low density could be charged, following other authors [26,27], to the physical interpretation of experimental data. In fact, we observed that the character of dielectric relaxation is quite far from the one given by the Debye theory approach (8) at low densities and/or high temperatures, i.e., for dilute systems in general, as those considered in this work (see Figs. 8–10). Alternatively, MD results should be compared with Raman [41] or far-infrared spectroscopy data [42] instead of microwave data. One way to do it could be through the measure of spectral shifts produced in measured spectra of SCW at different regimes.

We report a series of spectral densities [43] of SCW in the librational region in Fig. 12. The influence of density is already seen in the diffusion of water molecules in SCW, given by $S_H(0)$, which is much larger in the low-density states. The main band detected, around 180 $\mathrm{cm^{-1}}$ at the lowest density, shifts forward to 220 $\mathrm{cm^{-1}}$ at 0.3 $\mathrm{g\,cm^{-3}}$ and to about 300 $\mathrm{cm^{-1}}$ at 0.7 $\mathrm{g\,cm^{-3}}$. This band is located about 500 $\mathrm{cm^{-1}}$ in water at ambient conditions and it was attributed to librational motions of water molecules [45]. The importance of temperature changes is minor, observing some frequency displacements in all density ranges studied. Remarkably, we observe a redshift of the maximum of $S_H(\omega)$ as temperature increases that was also experimentally observed by Tassaing *et al.* [42] by means of far-infrared spectroscopy measurements in the range 25–240 °C.

VI. RESIDENCE TIMES

The last result analyzed in this study concerns the residence time τ_{res} of water molecules in the shell of its first neighbors in SCW, again as a function of density and temperature. A residence time correlation function $C_{res}(t)$ can be defined for a given molecule as the number of water molecules located in its first coordination shell which remain in the shell during a time *t*. Assuming an exponential behavior of $C_{res}(t)$ at long times, the residence time can be obtained as [46]

$$C_{res}(t) \approx \exp\left\{\frac{-t}{\tau_{res}}\right\}. \tag{10}$$

The results for τ_{res} are presented in Fig. 13. Again a two-regime behavior for densities below and above 0.1 $\mathrm{g\,cm^{-3}}$ is observed. In all cases, the time of residence of water molecules is higher for lower temperatures. This should be related with diffusion of water in SCW states, which is larger at high temperatures [19]. In the low-density states, namely, 0.01 $\mathrm{g\,cm^{-3}}$, τ_{res} grows significantly up to 4.5 times the value found at 0.1 $\mathrm{g\,cm^{-3}}$ at 650 K. Our findings are in good agreement with the tendency found in quasielastic incoherent neutron scattering experiments by Tassaing and Bellissent-Funel [47], who observed that residence times of water in SCW increase slightly for decreasing densities in the range 0.2–0.9 $\mathrm{g\,cm^{-3}}$.

As temperature rises, the increase of τ_{res} is slightly smaller. This is an indication of the gaslike behavior of low-density SCW, i.e., water structure is that of a clustered liquid

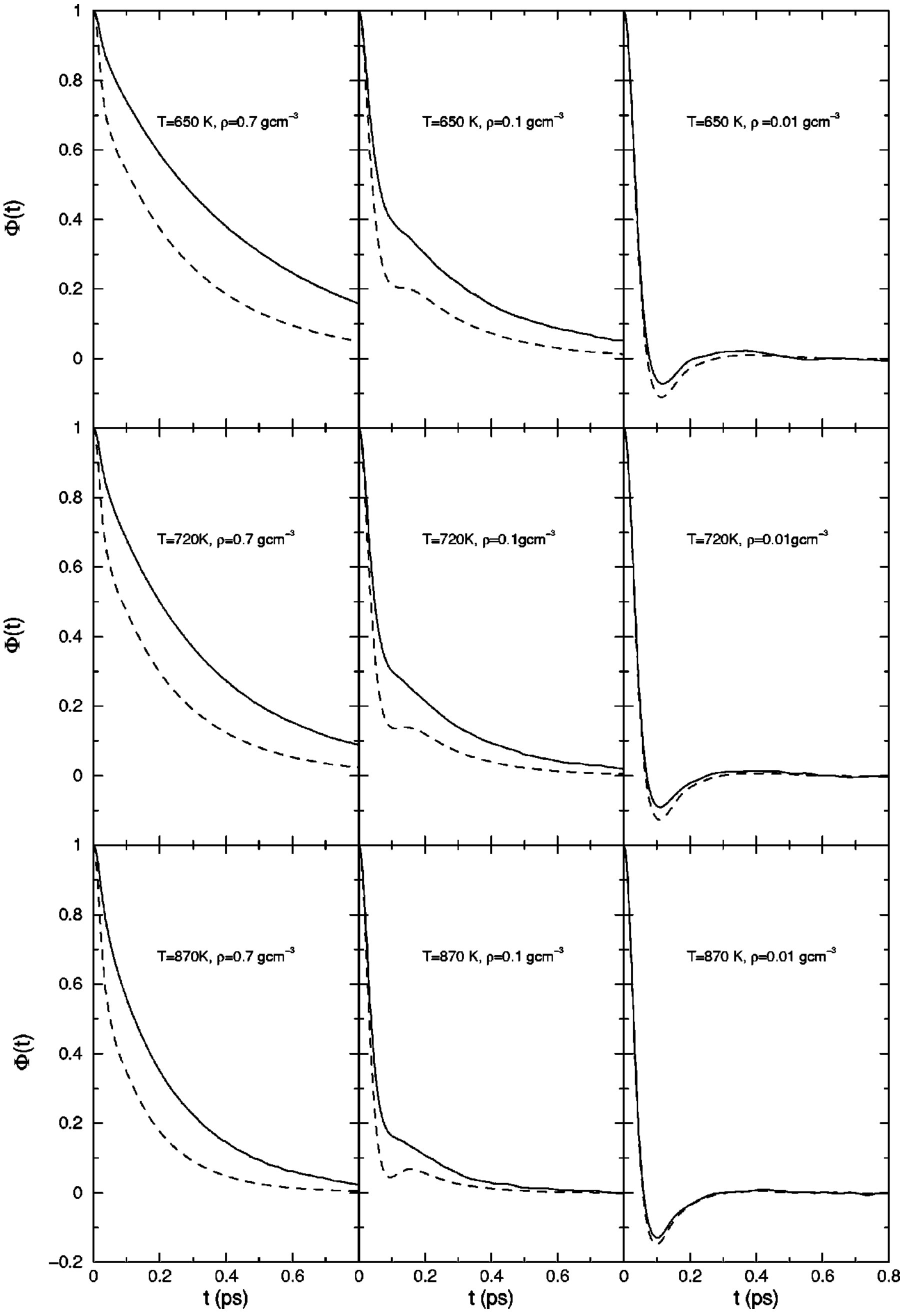

FIG. 8. Total (solid line) and single (dashed line) dipole moment autocorrelation functions at different temperatures and densities.

that has a diluted second coordination shell and this produces long residence times of water molecules in the first hydration shell. At higher temperatures, the combined increase of reorientational and translational diffusion (see Figs. 6 and 12) allows water molecules to promote easiely to second shells. This diffusive mechanism is well known at ambient conditions [48,49], when a water molecule migrates from the first to the second coordination shell, it spends some time on the first shell forming and breaking HB with neighboring companions, then undertakes a rotational diffusive motion including an HB breaking and, finally, moves to the second shell by translational diffusion. We see that this mechanism can work also in low-density SCW, provided that the HB network is weaker and diffusion is larger than in room temperature water, i.e., producing longer diffusion periods or larger τ_{res}. In addition, the relationship to the degree of hydrogen bonding supports this interpretation: both Raman spectrum measurements [50] and MD simulations (see Ref. [19] and references therein) have shown that in dense SCW states, the number of hydrogen bonds is still about 30% of that of water at ambient conditions. Further, the HB lifetime is markedly smaller in a SCW ambient [21] (about five times shorter than in water at room temperature). The reduced hydrogen bonding structure and the fast HB dynamics favors the reduction of residence times and the increase of water diffusion.

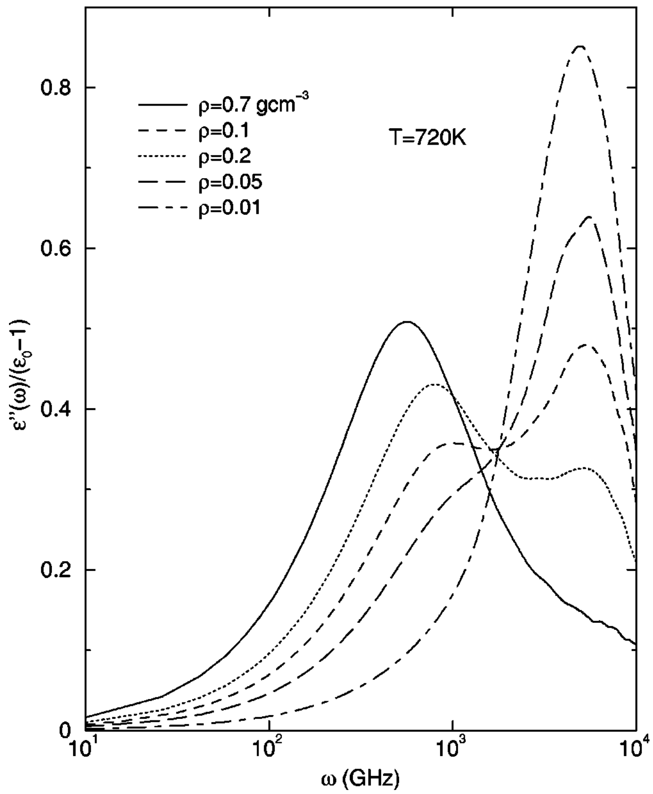

FIG. 9. Density dependence of the imaginary part of the frequency dependent dielectric constant.

VII. CONCLUDING REMARKS

A detailed study of orientational and dielectric properties of SCW has been performed by means of MD simulations. The SPC/E interacting potential assumed has revealed to be appropriate to model water in supercritical states in a wide range of temperatures and densities. We have observed that reorientational times of water molecules are in overall good agreement with NMR data and they are reduced by increasing the temperature, showing a two-regime behavior at very low densities (below 0.1 $\mathrm{g\,cm^{-3}}$), the characteristic reorientational times rise quickly with decreasing density but at densities above 0.1 $\mathrm{g\,cm^{-3}}$, the increase of such reorientational

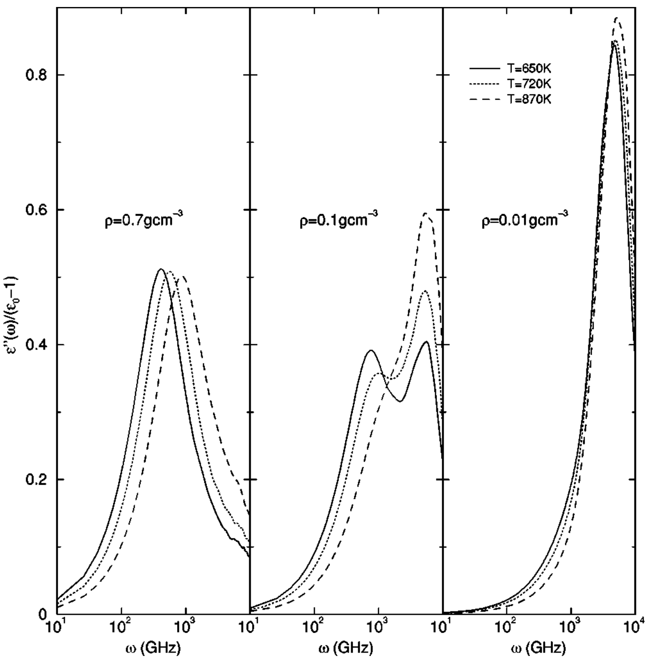

FIG. 10. Temperature dependence of the imaginary part of the frequency dependent dielectric constant.

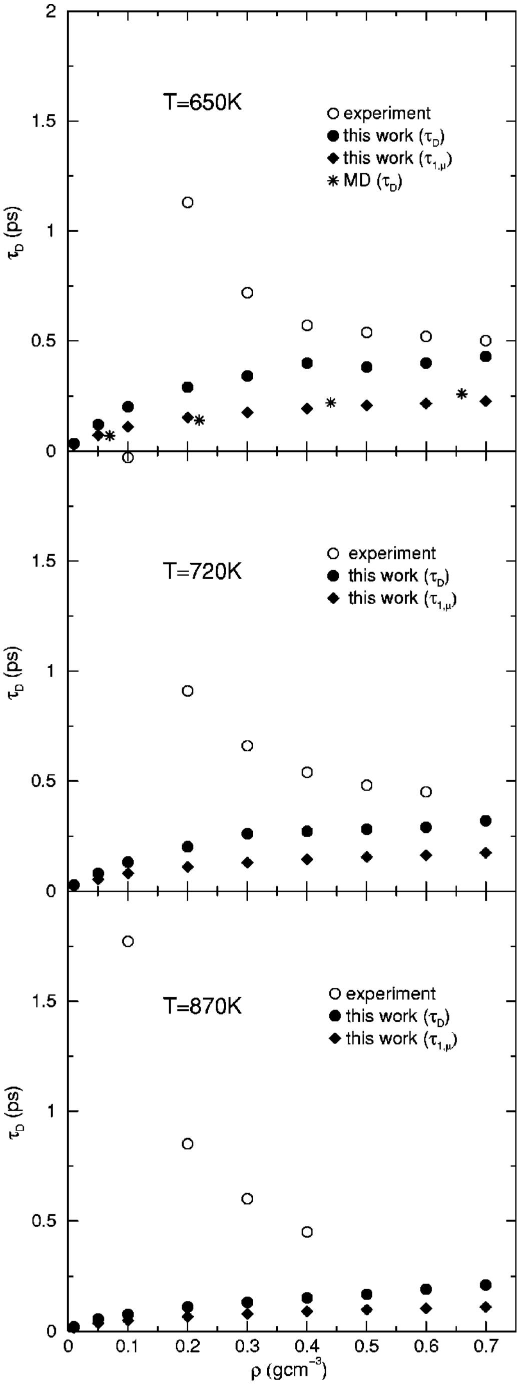

FIG. 11. Dielectric relaxation times as a function of density at different temperatures. Full circles—this work, open circles—MD results from Ref. [26], stars—microwave data [24], diamonds—single dipole moment reorientational times.

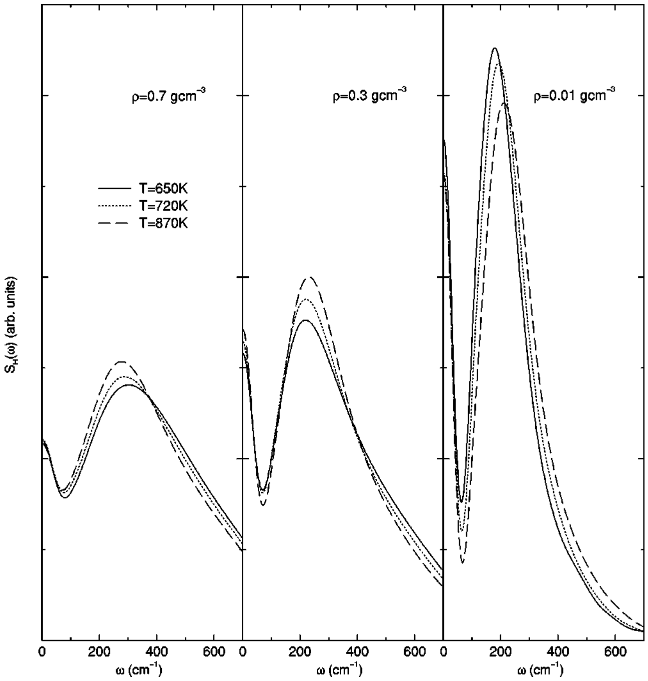

FIG. 12. Spectral densities of hydrogen atoms as a function of temperature at different densities.

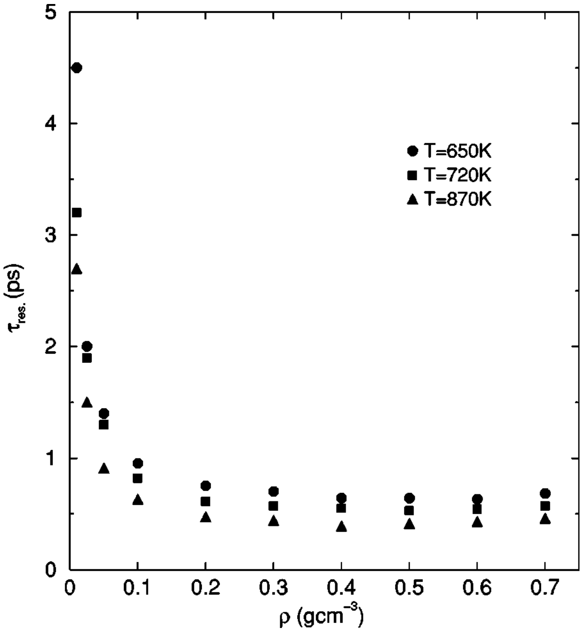

FIG. 13. Residence times of a water molecule in its first coordination shell as a function of density at different temperatures.

times is roughly linear for rising densities. Anisotropy in the molecular rotational motions has been also found at low densities.

Concerning dielectric relaxation, we have found discrepancies between microwave experiments and MD simulations, for Debye relaxation times at low density. This could be due to the fact that the experimental time measured is not exactly the same property computed in our simulations. Furthermore, residence times of water molecules in the first hydration shell show a behavior qualitatively similar to reorientational times. This fact, together with structural and dynamic data previously reported, reinforces an interpretation of the diffusive mechanism employed by water molecules during transitions from internal to external coordination shells: it would consist of a first stage based on rotational motions of the water molecule which can produce an HB breaking and a second stage associated with pure translational diffusion.

ACKNOWLEDGMENTS

The authors thank the Direcció General de Recerca de la Generalitat de Catalunya, for Grant No. 2001SGR-00222 and the Ministerio de Educación, Cultura y Deporte of Spain for Grant No. BFM2000-0596-C03-02.

[1] C.A. Eckert, B.L. Knutson, and P.G. Debenedetti, Nature (London) **383**, 313 (1996).
[2] J.B. Hanay and J. Hogarth, Proc. R. Soc. London, Ser. A **29**, 324 (1879).
[3] E.U. Franck and K. Roth, Faraday Discuss. Chem. Soc. **43**, 108 (1967).
[4] W.J. Lamb, G.A. Hoffman, and J. Jonas, J. Chem. Phys. **74**, 6875 (1981).
[5] N. Matubayashi, C. Wakai, and M. Nakahara, J. Chem. Phys. **107**, 9133 (1997).
[6] M.M. Hoffmann and M.S. Conradi, J. Am. Chem. Soc. **119**, 3811 (1997).
[7] T. Tassaing, M.-C. Bellissent-Funel, B. Guillot, and Y. Guissani, Europhys. Lett. **42**, 265 (1998).
[8] A. Botti, F. Bruni, M.A. Ricci, and A.K. Soper, J. Chem. Phys. **109**, 3180 (1998).
[9] M.A. Ricci, M. Nardone, A. Fontana, C. Andreani, and W. Hahn, J. Chem. Phys. **108**, 450 (1998).
[10] N. Matubayashi, N. Nakao, and M. Nakahara, J. Chem. Phys. **114**, 4107 (2001).
[11] A. Luzar, J. Chem. Phys. **113**, 10 663 (2000).
[12] R.D. Mountain, J. Chem. Phys. **90**, 1866 (1989).
[13] P.T. Cummings, H.D. Cochran, J.M. Simonson, R.E. Mesmer, and S. Karaborni, J. Chem. Phys. **94**, 5606 (1991).
[14] E.S. Fois, M. Sprik, and M. Parrinello, Chem. Phys. Lett. **223**, 411 (1994).
[15] T.I. Mizan, P.E. Savage, and R.M. Ziff, J. Phys. Chem. **100**, 403 (1996).
[16] A.G. Kalinichev and J.D. Bass, J. Phys. Chem. A **101**, 9720 (1997).
[17] P. Jedlovszky, J.P. Brodholt, F. Bruni, M.A. Ricci, A.K. Soper, and R. Vallauri, J. Chem. Phys. **108**, 8528 (1998).
[18] N. Yoshii, H. Yoshie, S. Miura, and S. Okazaki, J. Chem. Phys. **109**, 4873 (1998).
[19] J. Martí, J. Chem. Phys. **110**, 6876 (1999).
[20] M. Boero, K. Terakura, T. Ikeshoji, C.C. Liew, and M. Par-

rinello, Phys. Rev. Lett. **85**, 3245 (2000).

[21] J. Martí, Phys. Rev. E **61**, 449 (2000).

[22] F. Franks in *Water: A Comprehensive Treatise*, edited by F. Franks, (Plenum Press, New York, 1972), Chap. 1, Vol. 1.

[23] E. Guàrdia and J. Martí, J. Mol. Liq. **101**, 137 (2002).

[24] K. Okada, M. Yao, Y. Hiejima, H. Kohno, and Y. Kajhara, J. Chem. Phys. **110**, 3026 (1999).

[25] M.S. Skaf and D. Laria, J. Chem. Phys. **113**, 3499 (2000).

[26] C.N. Yang and H.J. Kim, J. Chem. Phys. **113**, 6025 (2000).

[27] B. Guillot and Y. Guissani, J. Chem. Phys. **114**, 6720 (2001).

[28] H.J.C. Berendsen, J.R. Grigera, and T.P. Straatsma, J. Phys. Chem. **91**, 6269 (1987).

[29] B. Guillot and Y. Guissani, J. Chem. Phys. **98**, 8221 (1993).

[30] M.C. Bellissent-Funel, T. Tassaing, H. Zao, D. Beysens, B. Guillot, and Y. Guissani, J. Chem. Phys. **107**, 2942 (1997).

[31] C. Rønne, L. Thrane, P.O. Åstrand, A. Wallqvist, K.V. Mikkelsen, and S.R. Keiding, J. Chem. Phys. **107**, 5319 (1997).

[32] H.J.C. Berendsen, J.P.M. Postma, W.F. van Gunsteren, A. DiNola, and J.R. Haak, J. Phys. Chem. **81**, 3684 (1984).

[33] J. Kestin and J.V. Sengers, J. Phys. Chem. Ref. Data **15**, 305 (1986).

[34] P. Maden and D. Kivelson, Adv. Chem. Phys. **56**, 467 (1984).

[35] D. Lankhorst, J. Schriever, and J.C. Leyte, Ber. Bunsenges. Phys. Chem. **86**, 215 (1982).

[36] W.A. Steele, Adv. Chem. Phys. **34**, 1 (1976).

[37] S.W. de Leeuw, J.W. Perram, and E.R. Smith, Annu. Rev. Phys. Chem. **37**, 245 (1986).

[38] M. Uematsu and E.U. Franck, J. Phys. Chem. Ref. Data **9**, 1291 (1980).

[39] M. Neumann, O. Steinhauser, and G.S. Pawley, Mol. Phys. **52**, 97 (1984).

[40] M. Neumann, J. Chem. Phys. **85**, 1567 (1986).

[41] G.E. Walrafen, M.R. Fisher, M.S. Hokmabadi, and W.-H. Yang, J. Chem. Phys. **85**, 6970 (1986).

[42] T. Tassaing, Y. Danten, and M. Besnard, J. Mol. Liq. **101**, 149 (2002).

[43] $S_H(\omega)$ in Fig. 11 have been computed as the Fourier transforms of the hydrogen velocity autocorrelation functions. See more details of the calculations elsewhere [23,44].

[44] J. Martí, E. Guàrdia, and J.A. Padró, J. Chem. Phys. **101**, 10 883 (1994).

[45] J. Martí, J.A. Padró, and E. Guàrdia, J. Chem. Phys. **105**, 639 (1996).

[46] R.M. Impey, P.A. Madden, and I.R. McDonald, J. Phys. Chem. **87**, 5071 (1983).

[47] T. Tassaing and M.-C. Bellissent-Funel, J. Chem. Phys. **113**, 3332 (2000).

[48] A. Luzar and D. Chandler, Nature (London) **379**, 55 (1996).

[49] A. Luzar and D. Chandler, Phys. Rev. Lett. **76**, 928 (1996).

[50] G.E. Walrafen, W.-H. Yang, and Y.C. Chu, J. Phys. Chem. B **103**, 1332 (1999).